Biomedical Physics & Engineering Express

PAPER

Spectral-detector based x-ray absorptiometry (SDXA): *in-vivo* bone mineral density measurements in patients with and without osteoporotic fractures

Alexis Laugerette[1,2], **Thomas Baum**[3], **Alexandra S Gersing**[1], **Benedikt J Schwaiger**[4], **Kevin Brown**[5], **Lena C Frerking**[6], **Nadav Shapira**[7], **Daniela Pfeiffer**[1], **Ernst J Rummeny**[1], **Roland Proksa**[6], **Franz Pfeiffer**[1,2,8] **and Peter B Noël**[1,7]

[1] Department of Diagnostic and Interventional Radiology, Department of Diagnostic and Interventional Radiology, School of Medicine & Klinikum rechts der Isar, Technical University of Munich, 81675 München, Germany
[2] Chair of Biomedical Physics, Department of Physics and Munich School of BioEngineering, Technical University of Munich, 85748 Garching, Germany
[3] Section of Diagnostic and Interventional Neuroradiology, School of Medicine & Klinikum rechts der Isar, Technical University of Munich, 81675 München, Germany
[4] Department of Neuroradiology, School of Medicine, Klinikum rechts der Isar, Technical University of Munich, München, Germany
[5] Philips Healthcare, Cleveland, OH, United States of America
[6] Philips Research Laboratories, Hamburg, Germany
[7] Department of Radiology, Perelman School of Medicine, University of Pennsylvania, Philadelphia, United States of America
[8] Institute for Advanced Study, Technical University of Munich, 85748 Garching, Germany

E-mail: Peter.Noel@pennmedicine.upenn.edu

Keywords: dual-energy x-ray absorptiometry, bone density, osteoporosis, spine, dual-energy computed tomography (DECT), spectral computed tomography, multidetector computed tomography (MDCT)

OPEN ACCESS

RECEIVED
2 April 2020

REVISED
27 July 2020

ACCEPTED FOR PUBLICATION
31 July 2020

PUBLISHED
24 August 2020

Abstract

Objectives: To study whether a dual-layer spectral CT scout scan-based areal BMD estimation method, called Spectral-detector based x-ray absorptiometry (SDXA), can differentiate patients with versus without osteoporotic fractures. *Methods:* The ability of the method to differentiate patients with osteoporosis was evaluated by assessing the areal BMD at the spine (L1 to L4) in a group of 19 patients presenting at least one fracture and comparing these results to the areal BMD of age- and gender-matched controls (57 patients). Finally, the reproducibility of SDXA was evaluated *in-vivo* through the calculation of coefficients of variation (CV), using three repeated analyses performed on each patient. *Results*: The average areal BMD of patients presenting fractures, measured with the scout scan-based method ($0.86 \pm 0.17\ g\ cm^{-2}$), was found to be significantly lower than the average BMD of the control group ($1.00 \pm 0.17\ g\ cm^{-2}$, $p = 0.043$). The reproducibility of the method *in-vivo* was found to be reasonable, with CVs ranging between 3.1 and 6.9%. *Conclusions*: The results illustrate that the SDXA method for DXA-equivalent areal BMD estimation -delivers the ability to distinguish patients presenting osteoporotic fractures. Considering the total number of CT examinations worldwide, SDXA could develop to be a useful tool for truly opportunistic osteoporosis screening for a future clinical day-to-day routine.

Abbreviations

SDXA	Spectral-detector based x-ray absorptiometry
BMD	Bone mineral density ($mg\ ml^{-1}$), sometimes also used for areal bone mineral density (aBMD, $g\ cm^{-2}$)
IV	Intra-venous (contrast agent)
DEXA	Dual-energy x-ray absorptiometry
AP	Antero-posterior
HA	Calcium-Hydroxyapatite, the main mineral component of bone

ESP	European spine phantom
CV	Coefficient of variation
VMSI	Virtual mono-energetic scout image

Introduction

Osteoporosis is a skeletal disorder defined by reduced bone density, altered bone quality and architecture, that increases the overall risk of low-impact and fragility fractures [1, 2]. It is estimated that osteoporosis affects over 75 million people in western countries (Europe, USA and Japan), with 3,5 million estimated new osteoporotic fractures each year in Europe alone (expected increase until 2025 by 28%), with the majority of these being hip and vertebral fractures [3, 4].

The current clinical standard for the diagnosis and monitoring of osteoporosis is dual-energy x-ray absorptiometry, abbreviated DXA [5–9]. It uses two x-ray spectra with different mean energies (respectively a low- and a high-energy spectrum) to compute the areal bone mineral density (aBMD, or simply BMD) at sites of interest, mainly the hip and the lumbar spine (vertebrae L1 to L4) [6, 8]. DXA results proved to correlate well with the bone status, with low DXA-aBMD being a predictor for a higher fracture risk [10]. However, osteoporosis is still an underdiagnosed and undertreated condition, with only about 30% of women and less than 5% of men being examined by central DXA at least once in their lives [11]. This could be explained by e.g. the limited availability of bone densitometers, as well as restrictions in personnel permitted to perform scans, a low awareness of the usefulness of BMD testing, and limited or even nonexistent reimbursement policies for DXA examinations [12].

The recent introduction of dual-layer detector CT scanners [13, 14] and upcoming introduction of photon-counting CT [15] could bridge this gap and offer new possibilities to identify patients with high fracture risk. Considering the large availability of CT scanners worldwide and number of CT examinations performed, opportunistic BMD measurements from CT datasets could be very beneficial for the detection of patients with osteoporosis. Options using volumetric data from CT scanners, either single- or dual-energy, or even PET/CT scanners were investigated previously [16–19]. While providing acceptable accuracy and reproducibility as well as volumetrically assessed trabecular BMD measurements, which are known to show a higher metabolic activity and are thus more prone to being influenced by bone density changes, these methods could suffer from low automatization capability and poor workflow integration. Moreover, intravenous (IV) contrast agent might be applied, compromising the BMD measurements with these techniques. Recently, another method called Spectral-Detector based x-ray Absorptiometry (SDXA), based on 2D dual-layer spectral CT scout scans, also called topograms, was developed and evaluated on standardized phantoms [20]. This study showed a substantial agreement with DXA and suggested that SDXA could provide DXA-equivalent BMD measurements. Considering that the scout scan is a mandatory part of each CT examination, and is obtained before a potential IV contrast injection, the application of this method *in-vivo* could be beneficial and enable a truly opportunistic osteoporosis screening, as well as enabling a better utilization of the radiation dose associated with scout scans [21–23].

Therefore, purpose of this study was to assess whether SDXA could differentiate patients with osteoporotic fractures from age- and gender-matched controls without fractures.

Materials and methods

Patient selection criteria

Institutional review board approval was obtained (institutional review board blinded for review) from the local ethics commission (Ethics Commission of the Medical Faculty, Technical University of Munich, Germany), and all analyses were performed in accordance with relevant institutional and legislative guidelines and regulations. Written informed consent was waived for this retrospective analysis of routinely acquired imaging data by the local ethics commission. All patients scanned between October 2017 and May 2018 with one dual-layer CT (IQon Spectral CT, Philips Healthcare) were selected according to two selection criteria: Firstly, dual-layer frontal scout scan raw data of (at least) the lumbar spine, with no spondylodesis or other foreign material, had to be available. Secondly, no oral contrast agent was present in the patient's abdomen, since oral contrast agent is usually applied before the scout scan and is known to largely affect the BMD determination. In total, 141 patients were identified with respect to these criteria. Among these, 10 female patients presented with at least one osteoporotic vertebral fracture (67 $\pm$ 10 years old). Similarly, 5 female patients (65 $\pm$ 14 years old) and 4 male patients (63 $\pm$ 8.3) presented with vertebral fractures due to multiple myeloma (MM). This patient group consisting of 19 patients in total was named the 'fracture group' in the following. For each patient of the 'fracture group', 3 age- and gender-matched control patients without any bone disease (e.g. osteoporosis or fracture), were randomly identified and selected following the above-mentioned criteria. All analysed scout scan data was acquired with a standard tube voltage of 120 kV and a standard scout scan tube current of 30 mA.

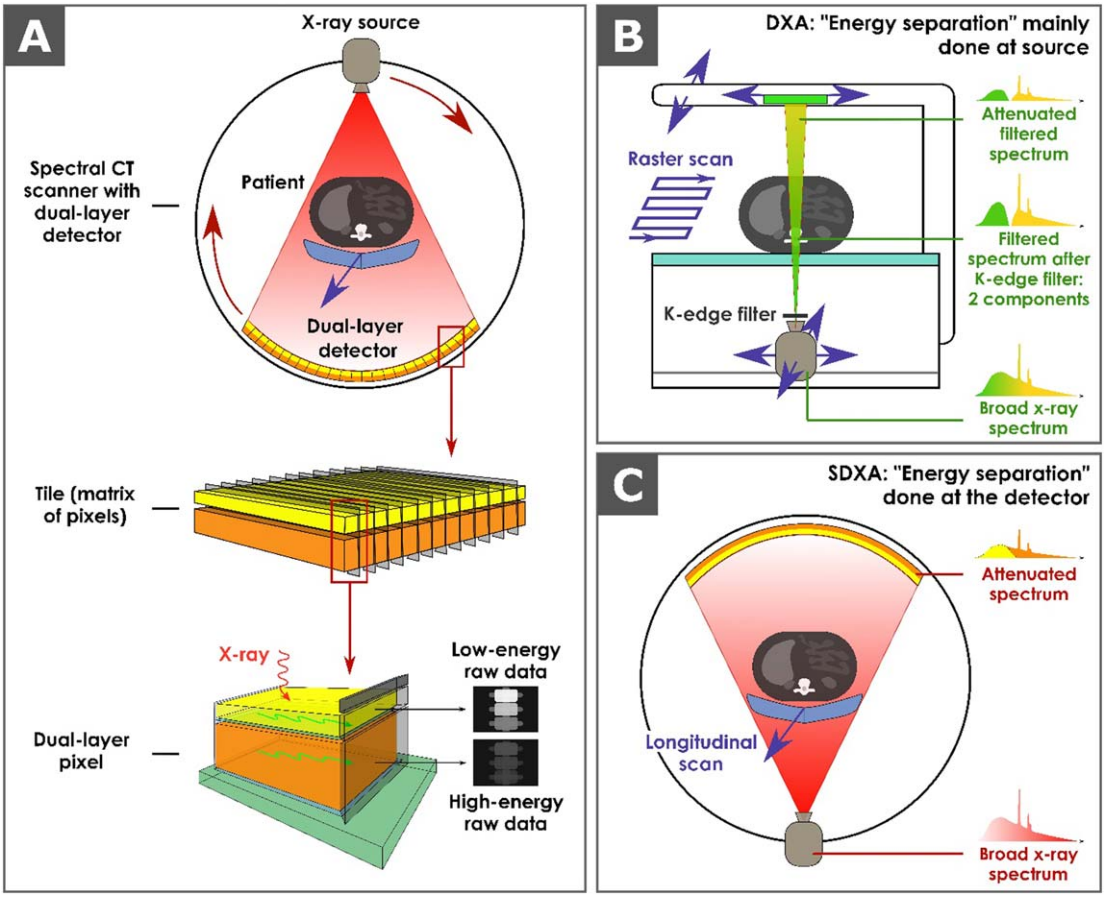

Figure 1. (A) Working principle of a dual-layer detector CT scanner. The detector is made of tiles, which are arrays of pixels. Each pixel is composed of a stack of two scintillator layers, converting respectively low-energy x-ray photons (top layer, yellow) and high-energy x-ray photons (bottom layer, orange) to visible light that is detected by standard side-looking photodiode arrays (grey), giving rise to low- and high-energy raw data. The whole assembly is supported by an application-specific integrated circuit (ASIC, green). (B) Geometry of a modern DXA scanner, with the x-ray source equipped with a K-edge filter, emitting a dual-energy narrow fan beam, firing up towards a photon-counting detector. The patient spine is imaged by a fine raster, the patient laying supine. This generally implies very low radiation exposure and typically leads to high image resolution and good energy separation, enabling an easy and efficient segmentation of bone contours for BMD determination. (C) Acquisition geometry used for the presented SDXA method and generally for standard CT scout scan protocols using the dual-layer spectral CT scanner. The x-ray source is positioned below the patient, lying supine, and emits an x-ray broad-spectrum fan beam up towards a dual-layer detector which follows detection principles described in (A). The patient is scanned longitudinally, without raster. This typically allows very short scanning times (<3 s), but decreases the image resolution due to magnification effects.

Spectral-detector based x-ray absorptiometry (SDXA)

The SDXA method utilizing dual-layer scout scan raw data was previously developed and provided excellent results for standard phantom measurements [20]. SDXA is designated as DXA-equivalent because it uses the same concepts as standard DXA devices to compute areal BMD values at the spine (vertebrae L1 to L4), which are expressed in the same, DXA-standard units ($g\,cm^{-2}$). Figure 1 illustrates the dual-layer detector technology as well as image acquisition differences between DXA and SDXA. In particular, SDXA uses the same algorithm as DXA to compute BMD. A detailed description of the algorithm is available in the supplemental material of [20].

DXA and SDXA: common aspects and differences

As shown in figures 1(B), (C), DXA and SDXA follow similar geometry to acquire dual-energy images of the spine, with some technical differences. Especially, both DXA and SDXA use a source placed below the patient which fires up toward a detector.

Modern DXA systems use two types of technology to generate the dual-energy image, depending on the manufacturer, namely fast-voltage switching and K-edge filtering, the latter being the most commonly encountered and therefore the one depicted in figure 1. In both cases, a raster-approach is used to scan the patient spine using a narrow fan beam. Therefore, both techniques offer high spatial resolution comparable to radiography (less than 0.6 mm laterally) and insignificant magnification of the imaged object, as well as relatively short scanning times (generally $<$ 1 min for the spine).

Particularly, in a K-edge system, the x-ray source is equipped with a filter possessing a K-edge around 40 keV, splitting a single x-ray spectrum into a low and a high energy component. Typically, a constant tube

voltage of 80 to 100 kVp is used in combination with one or several rare earth filters like cerium and samarium. The mean energies of the obtained spectra are around 30 and 70 keV.

In SDXA, the use of a dual-layer spectral CT scanner implies a slightly different acquisition: The x-ray source, generally operated at a voltage of 120 kVp, generates a broad energy spectrum in the form of a fan beam which is fired up towards a dual-layer detector. The patient is scanned longitudinally and no raster-scanning is needed. This typically leads to shorter scanning times (<3 s) but slightly decreased image resolution due to magnification effects (about 1 mm).

Regarding computation of the BMD results, both DXA and SDXA follow the same approach as they base on a pair of low- and high-energy monochromatic images (SDXA uses a pair of monochromatic images at 50 and 200 keV).

In-vivo BMD measurements at vertebrae L1 to L4

For each patient of the fracture and control group, areal BMD was estimated at the four lumbar vertebrae L1 to L4 using the SDXA method. Each BMD analysis was repeated three times on each dataset in order to account for variations due to, for example, manual soft-tissue segmentation. Results were averaged over each group and computed for each lumbar vertebra of interest. Figure 2 shows typical scout images obtained for a 28-year-old female control patient, displaying the different segmented regions used for BMD computation simultaneously.

Statistical analysis

An *a priori* power analysis was performed to calculate the appropriate sample size of the study cohorts in order to analyse differences in BMD values for patients with and without vertebral fractures. Using typical DXA data [25] and considering, based on previously published phantom studies [20], that the SDXA method performs similarly, the mean areal BMD for female patients presenting fractures, i.e. likely similar to the BMD in the elderly, can be estimated to 0.97 ± 0.16 g cm^{-2}, versus 1.24 ± 0.14 g cm^{-2} for healthy, young subjects; The criterion for significance had been set at 0.05. Based on this data a comparison of the two groups was simulated and a sample size of at least 15 patients per group would achieve a power greater than 0.8. Hence, 19 patients were included in each group to ensure adequate group sizes.

BMD values are presented as mean and standard deviation (SD). A paired-sampled Wilcoxon signed ranks test was performed using the software package SPSS (IBM SPSS Statistics for Windows, Version 25.0., IBM Corp., USA) in order to compare the mean areal BMD between the 'fracture' and control group. A *p-value* of less than 0.05 was considered to indicate a significant difference.

Reproducibility

Using the three repeated analyses performed for each patient of both groups, an estimate of the *in-vivo* reproducibility of the method can be obtained, since variability can be introduced, for example, due to the automatic vertebra segmentation algorithm or, most importantly, due to the manually-defined soft-tissue segmentation. Therefore, using this data, root-mean-square errors (SD_{RMS}, g/cm^2) as well as mean coefficients of variation (CV_{SD}, %) were calculated for both groups, for each vertebra of interest, in order to obtain an initial estimate of the precision error of the technique [26].

Results

In-vivo BMD measurements

Table 1 presents the mean areal BMD (g cm^{-2}) obtained at vertebrae L1 to L4, both for the fracture and the control groups. Results are given as mean BMD $\pm$ standard deviation.

A box plot summarizing the areal BMD distributions is presented in figure 3. The mean areal BMD in the 'fracture' group (0.86 ± 0.17 g cm^{-2}) was significantly lower than the mean BMD of the control group (1.00 ± 0.17 g cm^{-2}, $p = 0.043$). A post-hoc power analysis with these values confirmed an achieved power better than 0.9 for this test.

Reproducibility

Coefficients of variation (CV_{SD}) and root-mean-square errors (SD_{RMS}) for each group and each vertebra of interest were calculated and are summarized in table 2. Coefficients of variation range from 3.1 to 6.9% for both groups, whereas a wider variability is generally observed for the fracture group (5.47%) in comparison to the control group (3.59%). The same observation was made for the root-mean-square error. This observation is coherent with the known fact that, for most densitometric techniques, osteoporotic subjects generally tend to have higher precision errors [26]. However, it has to be noted that our reproducibility calculations only take into account three repeated measurements on the same patient datasets. Computing true reproducibility requires to scan the same patients multiple times in a row in a short amount of time. Since such data is not yet available, this study also does not claim to compute true short-term precision measures for SDXA, but only an initial estimate based on some influencing factors like segmentation quality, excluding, for example, patient positioning errors.

Discussion

In this study, the ability of the SDXA method to differentiate patients with versus without fractures was assessed *in-vivo*. The average BMD of the fracture

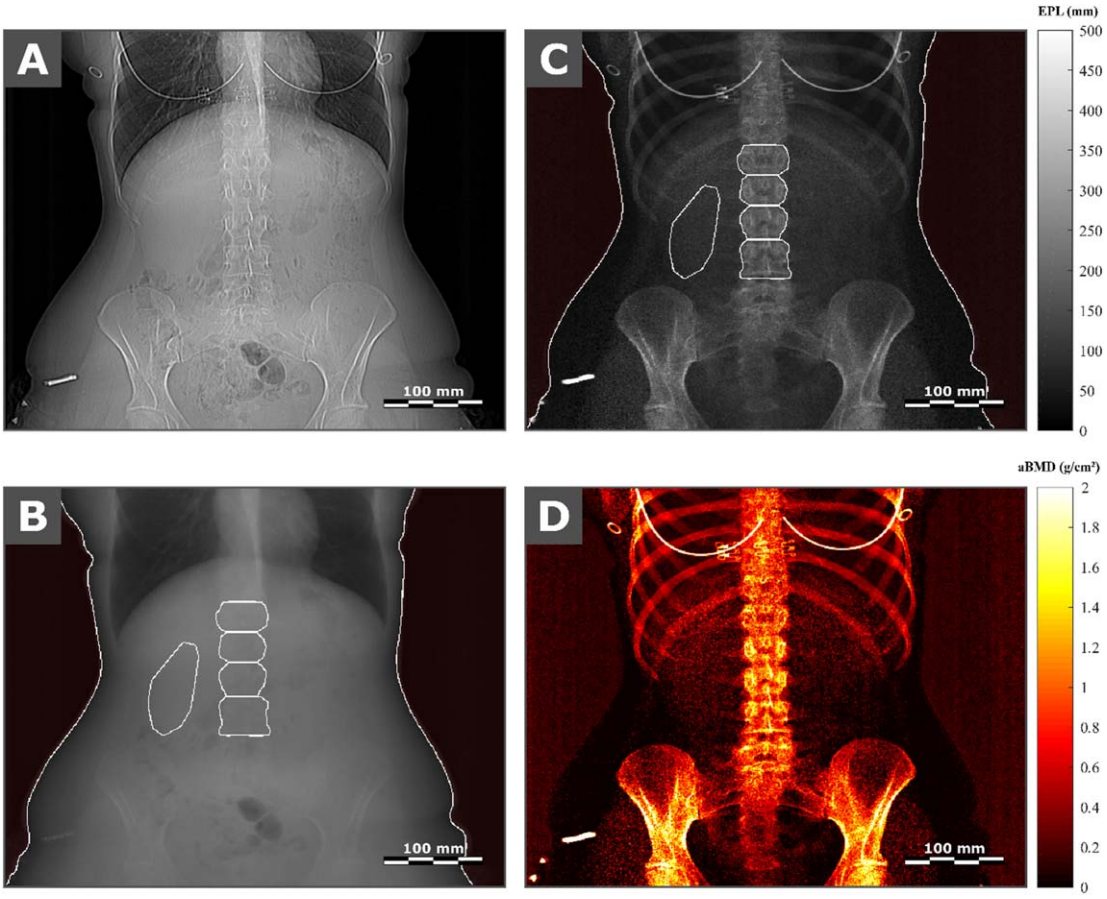

Figure 2. Typical scout images obtained for a 28-year-old female control patient. (A) Conventional scout image obtained as a weighted sum of the data from the two detector layers and equivalent to images generated by single-energy CT scanners. (B) A Compton-scatter-like scout image and (C) a photoelectric-like scout image generated from the pair of high- and low-energy raw data. The unit of (B) and (C) is mm and corresponds to equivalent path length (EPL) in a virtual object having Compton-scatter-like and photoelectric-like [24] attenuation properties of water. Images (B) and (C) show segmented regions used for the analysis, corresponding to vertebrae, soft-tissue and background. (D) DXA-equivalent areal BMD map expressed in g cm^{-2}, generated from the pair of Compton-scatter/photoelectric-like images.

Table 1. Absolute mean areal BMD results, expressed in g cm^{-2} as mean ± standard deviation, as measured for each vertebra of interest L1 to L4 in the 'fracture' and control groups. The last line L1_4 corresponds to results averaged over all four vertebrae.

	Mean BMD (g cm^{-2}) +/− STD	
Vertebra	Fracture group	Control group
L1	0.82 ± 0.19	0.88 ± 0.22
L2	0.87 ± 0.21	1.03 ± 0.16
L3	0.88 ± 0.21	1.04 ± 0.17
L4	0.90 ± 0.19	1.04 ± 0.21
L1_4	0.86 ± 0.17	1.00 ± 0.17

group was found to be significantly lower than the average BMD of the control group ($p = 0.043$). Moreover, initial estimates of reproducibility for the presented method were obtained, with CVs varying between 3.1%–6.9%. Here, it is worth to note that, since the reproducibility measures were obtained based on repeated measurements of the same patient datasets, this study does not present true short-term precision errors of SDXA.

The presented method based on spectral CT scout images may be considered an opportunistic osteoporosis screening tool since it may be applied to larger patient populations, overcoming the issue of DXA examinations with low participation rates due to various causes, such as lack of the awareness of the importance and availability of BMD testing [11, 27].

Numerous other techniques for opportunistic volumetric BMD measurements have been developed in the last years, based on routine MDCT data. For instance, BMD values derived from contrast-enhanced [12] as well as non-contrast-enhanced MDCT sagittal reformations [28] were shown to accurately differentiate patients with and without vertebral fractures. Similarly, a recent study showed that both synchronous and asynchronous phantom-based calibration as well as internal calibration could enable a reliable volumetric BMD estimation, even after intravenous contrast agent was applied [29]. Although they offer the advantage of not being altered by usual DXA-artifacts such as soft-tissue overlay or calcifications in the aorta, these 3D methods may suffer from a higher degree of required user interaction and might

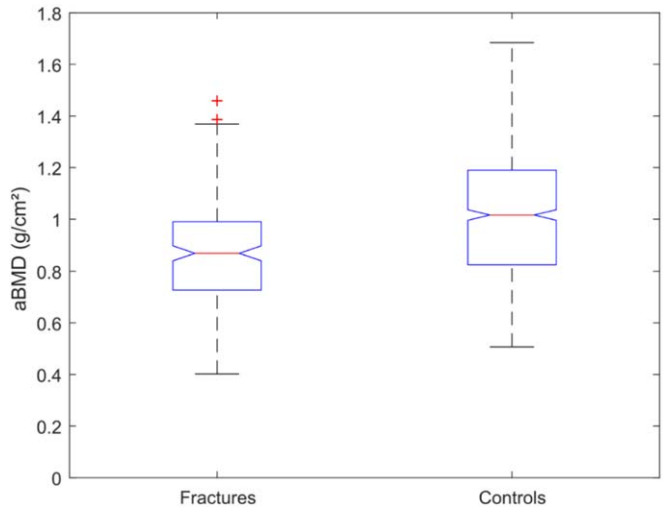

Figure 3. Box plot illustrating areal BMD results (g cm^{-2}) for the fracture group, consisting of 19 individuals, and the control group, matched 3:1 for age and gender with the fracture group. Red lines show group medians (fracture group: 0.87 g cm^{-2}; control group: 1.02 g cm^{-2}), blue boxes correspond to inter-quartile ranges IQR = Q3-Q1 (fracture group: [0.73;0.99] g cm^{-2}; control group [0.82;1.19] g cm^{-2}), and grey dashed lines correspond to the maximal data extent not considered as outlier, taking into account a maximum whisker length of w = 1.5 IQR (red crosses show data points considered outliers).

Table 2. (A) Standard deviation (SD_{RMS}) and (B) coefficients of variation (CV_{SD}) measured for each vertebra of interest (L1 to L4), in each patient group, showing the relatively good reproducibility of the method for this patient study and its robustness towards multiple, successive analyses. The column denoted 'mean' indicates the mean measures averaged over all vertebrae L1 to L4.

(A) SD_{RMS} (g cm^{-2})	L1	L2	L3	L4	mean
Control	0,037	0,034	0,033	0,041	0,036
Fracture	0,056	0,048	0,046	0,038	0,047
(B) CV_{SD} (%)	L1	L2	L3	L4	mean
Control	4,04	3,29	3,13	3,88	3,59
Fracture	6,86	5,59	5,17	4,23	5,47

therefore present a poor integration into the clinical workflow for screening purposes.

On the contrary, SDXA is novel in the sense that it makes use of 2D frontal scout images to compute a DXA-equivalent areal BMD. The technique previously showed precision, accuracy and linearity similar to modern DXA devices [20]. Further SDXA could be extended to any energy-resolving CT system (DECT, photon-counting CT), while non-detector-based solution would suffer from radiation dose and alignment penalties.

The technique could spark concerns regarding radiation exposure, since the absorbed doses during a scout scan for the selected patients were in the range 0.06–0.15 mGy, which is still higher than the typical dose associated with a routine DXA lumbar spine exam (0.037 mGy for a standard protocol at our institution). In particular, estimated effective doses for AP abdominal scout scans with the standard tube parameters used in this study (around 0.25 mSv) are still consequently higher than the effective dose of a DXA scan of the spine (around 0.013 mSv) [22, 30]. Nevertheless, the scout scan is always acquired in CT examinations and therefore, obtaining BMD measurements based on the scout image does not only represent an increase in radiation exposure, but above all a better, more meaningful utilization of the dose associated with scout procedures and CT procedures in general.

However, this study had limitations. The study showed that a scout scan-based method could differentiate patients with and without an increased fracture risk based on BMD measurements. Nonetheless, since data is not yet available, no *in-vivo* comparison between SDXA and the gold standard (DXA) or other, more novelBMD measurement techniques cited in this study (like volumetric, CT-based measurements) have yet been provided. This is currently under investigation for several comparisons. In addition, the presented reproducibility does not take into account successive patient repositioning, but only repeated analyses performed on the same datasets. Therefore, it may be that the true reproducibility of the method, including all sources of variation, for example patient positioning, might be higher. Moreover, the scout scan-based method uses a single large fan beam, and not a DXA-specific narrow fan beam. This is generally known to lead to more scatter radiation and less sharp images, which could increase the variability of the BMD results and the effectiveness of the segmentation process required to compute BMD.

In conclusion, BMD measurements based on SDXA can predict the fracture status, similarly to DXA. Considering the large number of CT scout scans performed worldwide, and the potential development and growing clinical acceptance of systems equipped with energy-resolving detectors, like dual-layer or

photon-counting CT scanners, the method evaluated in this work may provide a wide opportunistic BMD-testing program, simultaneously allowing a better utilization of the radiation dose associated with the scout scan.

ORCID iDs

Benedikt J Schwaiger https://orcid.org/0000-0003-1803-1510
Nadav Shapira https://orcid.org/0000-0002-9294-7001

References

[1] Guglielmi G 2013 Osteoporosis and bone densitometry measurements *Osteoporosis and Bone Densitometry Measurements* 41–55 978-3-642-27883-9
[2] Reiner B and Bertha F 2009 *Osteoporosis: Diagnosis,Prevention, Therapy* (Berlin: Springer)
[3] Hernlund E *et al* 2013 Osteoporosis in the European Union: Medical management, epidemiology and economic burden: a report prepared in collaboration with the International Osteoporosis Foundation (IOF) and the European Federation of Pharmaceutical Industry Associations (EFPIA) *Arch Osteoporos.* **8** 136
[4] Häussler B, Gothe H, Göl D, Glaeske G, Pientka L and Felsenberg D 2007 Epidemiology, treatment and costs of osteoporosis in Germany - The BoneEVA study *Osteoporos Int.* **18** 77–84
[5] Glüer C C 2016 30 years of DXA technology innovations *Bone.* **2017** 7–12
[6] Link T M 2012 Osteoporosis imaging: state of the art and advanced imaging *Radiology* **263** 3–17
[7] US Department of Health and Human Services 2004 Bone health and osteoporosis: a report of the Surgeon General *US Heal Hum Serv.* 437
[8] Bazzocchi A, Ponti F, Albisinni U, Battista G and Guglielmi G 2016 DXA: technical aspects and application *Eur. J. Radiol.* **85** 1481–92
[9] Bonnick S L 2008 Monitoring changes in bone density *Women's Heal.* **4** 89–97
[10] Lewiecki E M 2010 Bone densitometry and vertebral fracture assessment *Curr Osteoporos Rep.* **8** 123–30
[11] Curtis J R *et al* 2008 Longitudinal trends in use of bone mass measurement among older Americans, 1999–2005 *J. Bone Miner. Res.* **23** 1061–7
[12] Baum T *et al* 2012 Converted lumbar BMD values derived from sagittal reformations of contrast-enhanced MDCT predict incidental osteoporotic vertebral fractures *Calcif Tissue Int.* **90** 481–7
[13] McCollough C H, Leng S, Yu L and Fletcher J G 2015 Dual- and multi-energy CT: principles, technical approaches, and clinical applications *Radiology* [Internet] [cited 2018 Apr 17] **276** 637–53
[14] Vlassenbroek A 2011 Dual layer CT. In: dual energy CT in clinical practice *Medical Radiology* (Berlin, Heidelberg: Springer-Verlag) (https://doi.org/10.1007/978-3-642-01740-7)
[15] Willemink M J, Persson M, Pourmorteza A, Pelc N J and Fleischmann D 2018 Photon-counting CT: technical principles and clinical prospects *Radiology* **289** 172656
[16] Brett A D and Brown J K 2015 Quantitative computed tomography and opportunistic bone density screening by dual use of computed tomography scans *J. Orthop. Transl.* **3** 178–84
[17] Schwaiger B J *et al* 2017 Vertebral and femoral bone mineral density and bone strength in prostate cancer patients assessed in phantomless PET/CT examinations *Bone.* **101** 62–9
[18] van Hamersvelt R W *et al* 2017 Accuracy of bone mineral density quantification using dual-layer spectral detector CT: a phantom study *Eur Radiol.* **27** 4351–9
[19] Mei K *et al* 2017 Bone mineral density measurements in vertebral specimens and phantoms using dual-layer spectral computed tomography *Sci. Rep.* **7** 1–10
[20] Laugerette A *et al* 2019 DXA-equivalent quantification of bone mineral density using dual-layer spectral CT scout scans *Eur Radiol* **29** 4624–34 (http://link.springer.com/10.1007/s00330-019-6005-6)
[21] Patel A A, Maver D W and Siegel E L 2010 The CT Scout Exam: A survey of radiation dose, utilization, and opportunity for substantial dose reduction *Radiological Society of North America 2010 Scientific Assembly and Annual Meeting (Chicago)*
[22] Bohrer E, Schäfer S, Mäder U, Noël P B, Krombach G A and Fiebich M 2017 Optimierung der Strahlenbelastung von CT-Übersichtsaufnahmen *Z. Med. Phys.* [Internet] **27** 145–58
[23] Schmidt B, Saltybaeva N, Kolditz D and Kalender W A 2013 Assessment of patient dose from CT localizer radiographs *Med. Phys.* **40**
[24] Hua C, Shapira N, Merchant T E, Klahr P and Yagil Y 2018 Accuracy of electron density, effective atomic number, and iodine concentration determination with a dual-layer dual-energy computed tomography system *Med. Phys.* [Internet] [cited 2019 Sep 8] **45** 2486–97
[25] Mazess R B and Barden H 1999 Bone density of the spine and femur in adult white females *Calcif Tissue Int.* **65** 91–9
[26] Gluer C, Blake G, Lu Y, Blunt B A, Jergas M I and Genant H K 1995 Accurate assessment of precision Errors: How to measure the reproducibility of bone densitometry techniques *Osteoporos Int.* **5** 262–70
[27] Read M 1998 Osteoporosis in the European Community: A Call to Action (https://iofbonehealth.org/osteoporosis-european-community-call-action)
[28] Schwaiger B J, Gersing A S, Baum T, Noël P B, Zimmer C and Bauer J S 2014 Bone mineral density values derived from routine lumbar spine multidetector row CT predict osteoporotic vertebral fractures and screw loosening *Am. J. Neuroradiol.* **35** 1628–33
[29] Kaesmacher J, Liebl H, Baum T and Kirschke J S 2017 Bone mineral density estimations from routine multidetector computed tomography: a comparative study of contrast and calibration effects *J. Comput. Assist. Tomogr.* **41** 217–23
[30] Damilakis J, Adams J E, Guglielmi G and Link T M 2010 Radiation exposure inx-ray-based imaging techniques used in osteoporosis *Eur Radiol.* **20** 2707–14